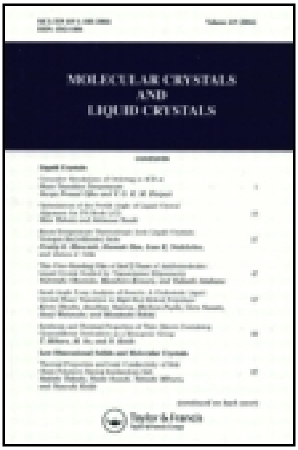

Molecular Crystals and Liquid Crystals Science and Technology. Section A. Molecular Crystals and Liquid Crystals

Publication details, including instructions for authors and subscription information:
http://www.tandfonline.com/loi/gmcl19

Numerical Studies of Ground State Phase Diagrams for the MMX Chains

Makoto Kuwabara [a] & Kenji Yonemitsu [a]

[a] Institute for Molecular Science, Okazaki, 444-8585, Japan

To cite this article: Makoto Kuwabara & Kenji Yonemitsu (2000): Numerical Studies of Ground State Phase Diagrams for the MMX Chains, Molecular Crystals and Liquid Crystals Science and Technology. Section A. Molecular Crystals and Liquid Crystals, 341:2, 533-538

To link to this article: http://dx.doi.org/10.1080/10587250008026194

Mol. Cryst. and Liq. Cryst., 2000, Vol. 341, pp. 533-538
Reprints available directly from the publisher
Photocopying permitted by license only

Numerical Studies of Ground State Phase Diagrams for the MMX Chains

MAKOTO KUWABARA and KENJI YONEMITSU

Institute for Molecular Science, Okazaki 444–8585, Japan

We study ground state phase diagrams for the MMX chains, using a one-dimensional dimerized 3/4-filled extended Hubbard-Peierls model with site diagonal and off-diagonal electron-lattice interactions. The ground states are obtained mainly in the Hartree-Fock approximation, and their accuracy is checked by the exact diagonalization of small clusters. We find a new phase in addition to frequently considered phases and compare our results with experimental results.

Keywords: MMX chain; dimerization; extended Hubbard-Peierls model

INTRODUCTION

The quasi-one-dimensional halogen-bridged metal complexes (MX and MMX chains) have strong electron-lattice (e-l) coupling and electron-electron (e-e) interaction and have attracted much interest. While the MX chains have been investigated experimentally[1,2] and theoretically[3-6] for a long time, the MMX chains started to be studied rather recently[7-12]. The MMX chains possess dimers of metal ions, and the dimer structure gives more variety in the electronic phases, compared with the MX chains. For example, $Pt_2(CH_3CS_2)_4I$ is metallic above 300K, although most of the MX and MMX chains are insulators[10,11]. The character of the metal-insulator (M-I) transition has not been clarified yet. In the MMX chains, the metal (M) and halogen (X) ions are easily displaced, and their displacements are closely connected with the electronic state. Various phases appear owing to competition between e-l and e-e interactions. Here we study ground state phase diagrams for the MMX chains.

MODEL

As a first step, we assume that the level of the X p_z orbital lies much lower than that of the M d_{z^2} orbital for simplicity, and we take a one-dimensional dimerized 3/4-filled model for d_{z^2} bands;

$$
\begin{aligned}
H = & -\sum_{i=1,\sigma}^{N} t_{\mathrm{MM}}\left(c^{\dagger}_{a,i,\sigma}c_{b,i,\sigma} + \text{h.c.}\right) - \sum_{i=1,\sigma}^{N}\left[t_{\mathrm{MXM}} - \alpha\left(y_{b,i} + y_{a,i+1}\right)\right]\left(c^{\dagger}_{a,i+1,\sigma}c_{b,i,\sigma} + \text{h.c.}\right) \\
& - \beta\sum_{i=1}^{N}\left(y_{a,i}n_{a,i} + y_{b,i}n_{b,i}\right) + U\sum_{i=1}^{N}\left(n_{a,i,\uparrow}n_{a,i,\downarrow} + n_{b,i,\uparrow}n_{b,i,\downarrow}\right) \\
& + \sum_{i=1}^{N}\left(V_{\mathrm{MM}}n_{a,i}n_{b,i} + V_{\mathrm{MXM}}n_{b,i}n_{a,i+1}\right) + V_2\sum_{i=1}^{N}\left(n_{a,i}n_{a,i+1} + n_{b,i}n_{b,i+1}\right) \\
& + \frac{K}{2}\sum_{i=1}^{N}\left(y_{a,i}^{2} + y_{b,i}^{2}\right),
\end{aligned}
$$

where $c^{\dagger}_{a,i,\sigma}$ ($c^{\dagger}_{b,i,\sigma}$) creates an electron with spin σ at site a (b) in the i-th dimer, $n_{a,i,\sigma}= c^{\dagger}_{a,i,\sigma}c_{a,i,\sigma}$ and $n_{a,i}=\sum_{\sigma} n_{a,i,\sigma}$. The unit cell consists of two M sites a and b, forming a dimer, and an X site. For the lattice degrees of freedom, we take the bond length (relative to that in the undistorted phase) $y_{a,i}$ ($y_{b,i}$) between the M site a (b) in the i-th unit cell and its neighboring X site. A change in the interdimer distance is described by $y_{b,i}+y_{a,i+1}$. We fix the distance between the M site within a dimer and the corresponding intradimer transfer integral t_{MM}.

The interdimer transfer integral through the X p_z orbital is assumed to depend on the interdimer distance linearly with coefficient α. The level of the M d_{z^2} orbital depends on the M-X bond length with coefficient β. U is the on-site repulsion. V_{MM} and V_{MXM} are the intradimer and interdimer nearest-neighbor repulsion, respectively. V_2 is the next-nearest-neighbor repulsion. K denotes the elastic constant. The periodic boundary condition is imposed.

RESULTS AND DISCUSSION

So far it is generally expected that there are four possible electronic states; (1) an averaged-valence (AV) state, (2) a charge-density-wave (CDW) state, (3) a charge-polarization (CP) state, and (4) an alternate-charge-polarization (ACP) state, as shown schematically in Fig. 1. In addition to these states, we find a new state (5). We call it a bond-charge-density-wave (BCDW) state. In the phase (1), the levels of the M d_{z^2} orbitals are spatially uniform and there are three electrons in a dimer unit (not shown). In the other states, the d_{z^2} levels deviate from the position in (1), depending on the X displacements. First we consider the atomic limit ($t_{MM} = t_{MXM} = \alpha = 0$). The site energy per two unit cells relative to that in (1) is stabilized by 2Δ for (2), (3) and (4), where Δ is the deviation of the d_{z^2} level. The new phase (5) is stabilized the most if Δ is fixed. In the phase (5), three of the four levels in the two dimers are lowered by Δ and fully occupied, while the rest is empty and lifted. Three of the four M-X bonds are stretched and the rest is shrunk to keep the system length constant. Charge density and bond-charge density are alternating when a dimer is viewed

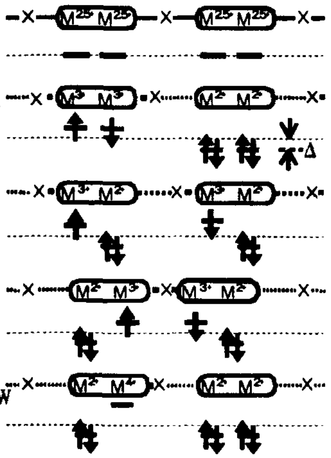

	ε	U	V_{MM}	V_{MXM}	V_2
(1) AV	0	-	-	-	-
(2) CDW	-2Δ	2	5	4	4
(3) CP	-2Δ	2	4	4	5
(4) ACP	-2Δ	2	4	5	4
(5) BCDW	-6Δ	3	4	4	4

FIGURE 1 Schematic electronic structures for the MMX chain. The partial energy per two units from each term is shown in the atomic limit(t_{MM}=t_{MXM}=α=0) for each phase: the site energy (ε), the on-site repulsion term (U), the intradimer and interdimer repulsion terms (V_{MM}, V_{MXM}), and the next-nearest-neighbor repulsion term (V_2).

as a unit.

In Fig. 2, we show ground state phase diagrams on the α - β plane for the three sets of e-e interaction strengths obtained in the Hartree-Fock (HF) approximation. In the noninteracting case [Fig. 2(a)], the CDW, ACP and BCDW phases are realized. When both α and β are weak, the CDW phase is stable. As α increases, the ACP phase becomes stable owing to the energy gain by the interdimer transfer. As β increases, Δ in Fig. 1 becomes large stabilizing the BCDW phase. The on-site repulsion stabilizes the AV and CP phases [Fig. 2(b)], while the nearest-neighbor and next-nearest-neighbor

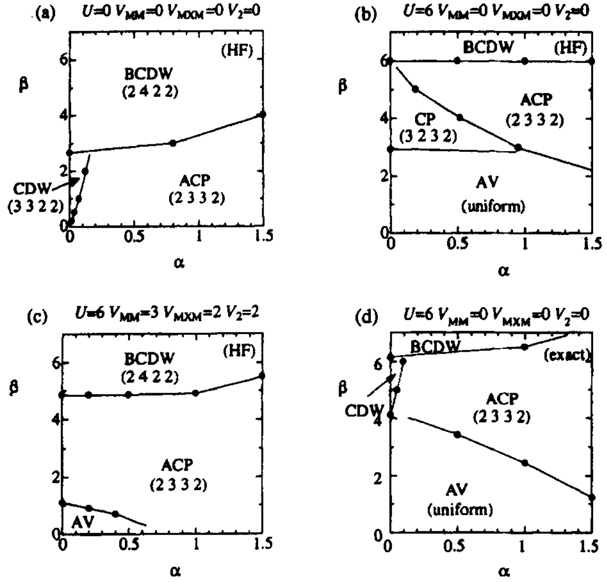

FIGURE 2 Ground state phase diagrams for (a) the noninteracting case; (b) U=6, $V_{MM}=V_{MXM}=V_2=0$; (c) U=6, $V_{MM}=3, V_{MXM}=2, V_2=2$ in the HF approximation for 120 M sites; and (d) U=6, $V_{MM}=V_{MXM}=V_2=0$ by the exact diagonalization for 12 M sites.

repulsion destabilizes them [Fig. 2(c)]. We have checked the accuracy of these phase diagrams by exactly diagonalizing the clusters of 12 sites. Qualitatively, the HF results give good agreement with the exact results except for the CP phase in Fig. 2(b). The AV, ACP, and CDW phases become stable instead of the CP phase there, as shown in Fig. 2(d). It has been experimentally observed that $Pt_2(CH_3CS_2)_4I$ has a valence state schematically represented by -X-M^{+2}-M^{+3}-X-M^{+3}-M^{+2}-X- (corresponding to the ACP phase in Fig. 1) below 80K and has finite magnetic susceptibility in low temperatures[10,11]. Our results show that the ACP phase is stable in some (α, β) region for any parameter set of the e-e interaction strengths. In the ACP phase, the electrons on M^{+3} sites of -X-M^{+2}-M^{+3}-X-M^{+3}-M^{+2}-X- form a singlet pair. We expect a small but finite spin gap in the ground state of $Pt_2(CH_3CS_2)_4I$. To explain the metallic property above 300K and to quantitatively estimate the spin gap, X p_z orbitals would be important. The consequent two-band model for the MMX chains will be studied elsewhere.

Acknowledgments

The authors thank H. Kitagawa, H. Okamoto, and S. Yamamoto for fruitful discussions. This work was supported by a Grand-in-Aid for Scientific Research on Priority Area "Metal-Assembled Complexes" and for Encouragement of Young Scientists from the Ministry of Education, Science Sports and Culture, Japan.

References

[1] M. Tanaka, S. Kurita, Y. Okada, T. Kojima, Y. Yamada, *Chem. Phys.* **96,** 343 (1985).
[2] H. Okamoto, Y. Kaga, Y. Shimada, Y. Oka, Y. Iwasa, T. Mitani, and M. Yamashita, *Phys. Rev. Lett.* **80,** 861 (1998).
[3] K. Nasu, *J. Phys. Soc. Jpn.* **52,** 3865 (1983), **53,** 302 (1984), **53,** 427 (1984).
[4] J. T. Gammel, A. Saxena, I. Batistic, A. R. Bishop, and S. R. Phillpot, *Phys. Rev. B* **45,** 6408 (1992).
[5] K. Iwano, *J. Phys. Soc. Jpn.* **66,** 1088 (1997).
[6] S. Yamamoto, *Phys. Lett. A* **247,** 422 (1998).
[7] M. Yamashita and K. Toriumi, *Inorg. Chim. Acta.* **178,** 143 (1990).
[8] N. Kimura, H. Ohki, R. Ikeda, and M. Yamashita, *Chim. Phys. Lett.* **220,** 40 (1994).
[9] T. Mitani, Y. Wada, M. Yamashita, K. Toriumi, A. Kobayashi, and H. Kobayashi, *Synth. Met.* **64,** 291 (1994).
[10] H. Kitagawa, N. Onodera, J.S. Ahn, T. Mitani, K. Toriumi, and M. Yamashita, *Synth. Met.* **86,** 1931 (1997).
[11] H. Kitawagta, N. Onodera, T. Sonoyama, M. Yamamoto, M. Fukawa, T. Mitani, M. Seto, and Y. Maeda, preprint.
[12] S. A. Borshch, K. Prassides, V. Robert, A. O. Solonenko, *J. Chem. Phys.* **100,** 4562 (1998).